Proc. Natl. Acad. Sci. USA
Vol. 88, pp. 10890–10894, December 1991
Immunology

Lymphocytes with a CD4$^+$ CD8$^-$ CD3$^-$ phenotype are effectors of experimental cutaneous graft-versus-host disease

(T cells/differentiation/bone marrow transplantation)

HIROHIKO SAKAMOTO*†, JAMES MICHAELSON‡§, WILLIAM K. JONES*†, ATUL K. BHAN‡§, SUNIL ABHYANKAR*†, MICHAEL SILVERSTEIN*†, DAVID E. GOLAN¶‖**, STEVEN J. BURAKOFF*†, AND JAMES L. M. FERRARA*†‡‡

*Division of Pediatric Oncology, Dana–Farber Cancer Institute and The Children's Hospital; ‖Division of Hematology, Brigham and Women's Hospital; and §Massachusetts General Hospital Cancer Center and Departments of †Pediatrics, ‡Pathology, ¶Biological Chemistry and Molecular Pharmacology, and **Medicine, Harvard Medical School, Boston, MA 02115

Communicated by H. Sherwood Lawrence, August 9, 1991 (received for review August 31, 1990)

ABSTRACT **Graft-versus-host disease (GVHD) is known to cause profound dysregulation of the immune system, although its effector mechanisms are poorly understood. We now describe an effector lymphocyte of unusual phenotype in the skin of mice with GVHD. This cell is of donor origin and expresses several T-cell surface proteins including Thy-1, CD2, and CD4 but does not express CD8, CD3, NK1.1, or macrophage antigens. Mononuclear cells of this phenotype are the predominant lymphocyte in the epidermis of mice with GVHD 3 weeks after transplant but are not detected in transplanted mice without GVHD. Isolation and transfer of these lymphocytes into secondary recipients causes epidermal damage characteristic of GVHD. These data demonstrate that CD4$^+$ CD8$^-$ CD3$^-$ lymphocytes are an important effector population that can be amplified outside the thymus and that can mediate target organ damage of GVHD.**

Graft-versus-host disease (GVHD) remains a major complication of allogeneic bone marrow transplantation. Mature T cells in the donor bone marrow initiate GVHD in immunocompromised or otherwise susceptible hosts (1–5). The afferent arm of GVHD, including the subsets of T cells required to initiate the reaction in response to various histocompatibility antigens, has been carefully studied (3–5). However, the constellation of target organs affected during clinical disease is unusual (skin, intestine, liver, immune system), and the nature of effector–target interactions is obscure (6).

To understand these interactions, we have studied the lymphocytes that appear in the skin during GVHD. The skin is a major GVHD target organ, and during acute GVHD the epidermis is primarily affected. In a well-defined murine model (7, 8), epidermal necrosis peaks early after transplant (week 3). These cells are Thy-1$^+$ and CD2$^+$, are of donor origin, and bear no macrophage markers. Recently, a similar population of CD4$^+$ CD8$^-$ CD3$^-$ thymocytes was described in normal thymus, which expands during periods of rapid thymocyte proliferation, such as during fetal ontogeny and after bone marrow transplantation (9–11). In addition, the earliest T-lineage precursor cells in the thymus express CD4 prior to rearrangement of T-cell receptor genes (12). Our data show that CD4$^+$ CD8$^-$ CD3$^-$ lymphocytes are also important effector cells of cutaneous GVHD.

MATERIALS AND METHODS

Transplantation and GVHD Induction. Ten- to 14-week-old CBA mice (The Jackson Laboratory) (n = 12) were lethally irradiated [1100 cGy in two doses separated by 3 hr; ^{137}Cs source: γ cell 40 (Nordion International, Ontario, Canada)] and transplanted with 10^7 B10.BR bone marrow cells that were depleted of T cells by two cycles of anti-Thy-1.2 and complement. GVHD was induced in seven mice by adding 10^6 nylon–wool-passaged B10.BR splenocytes (>80% Thy-1$^+$) to bone marrow.

Immunofluorescence Staining. Ear skin was harvested on the days indicated, split into two layers with a watchmaker's forceps, and incubated for 24 hr in L15 medium at room temperature to reduce nonspecific staining. Skin was then cut into 3 × 5 mm pieces, embedded in Tissue-Tek OCT compound (Miles), and immediately frozen at −50°C. Frozen blocks were stored in isopentane at −30°C and sectioned on a Reichert–Jung 2800 Frigocut E cryostat at −19°C. Four-micrometer sections were melted onto slides, dried for 30 min, fixed in acetone for 10 min, and washed three times in phosphate-buffered saline (PBS). Ten microliters of a 1:20 dilution of primary antibody (anti-CD2: RM2-2; anti-CD3: 145-2C11; anti-CD4: GK1.5; anti-CD8: 53.6; and anti NK1.1: PK136) containing 2% normal goat serum or 10 μl of a 1:50 dilution of fluorescein isothiocyanate (FITC)-conjugated anti-Thy-1.2 (New England Nuclear) was applied. Slides were incubated in a damp chamber for 45 min at 25°C and washed four times with PBS, and then 10 μl of second antibody [1:60 dilution of FITC-conjugated rabbit anti-rat immunoglobulin or FITC-conjugated goat anti-hamster immunoglobulin (for CD3)] was applied. Slides were again incubated in a damp chamber for 45 min at room temperature, washed four times with PBS, protected with coverslips (mounting solution: 1 ml of PBS, 9 ml of glycerine, and 10 mg of p-phenylamine diamine), and examined under an Axioplan fluorescence microscope (Zeiss). To quantitate positive cells per linear mm, cells in the epidermis were counted, and the length of each sample was measured with an ocular grid. Repeated analysis in a blinded fashion yielded results within 15% of initial scores. Two-color immunofluorescence was performed by simultaneous application of anti-CD3 and anti-CD4, followed by FITC-conjugated swine anti-hamster immunoglobulin and tetramethylrhodamine 5(and 6)-isothiocyanate (TRITC)-conjugated goat anti-rat immunoglobulin. Single-cell suspensions were stained for two-color immunofluorescence with FITC-conjugated anti-CD3 and phycoerythrin (PE)-conjugated anti-CD4.

Digital Analysis of Fluorescence Intensity. An ACAS 570 interactive laser cytometer (Meridian Instruments, Okemos, MI) was used to quantify CD3 and CD4 labeling on skin lymphocytes *in situ* by fluorescein-conjugated anti-hamster immunoglobulin and rhodamine-conjugated anti-rat immunoglobulin, respectively. The instrument was equipped with a

The publication costs of this article were defrayed in part by page charge payment. This article must therefore be hereby marked "*advertisement*" in accordance with 18 U.S.C. §1734 solely to indicate this fact.

Abbreviations: GVHD, graft-versus-host disease; FITC, fluorescein isothiocyanate.

‡‡To whom reprint requests should be addressed at: Dana–Farber Cancer Institute, 44 Binney Street, Boston, MA 02115.

5-W argon laser, inverted phase-contrast microscope, *x–y* microstepping stage, dual photomultiplier tube housing, and 386-based computer for experiment control and data analysis. Laser scan strength was 50 mW with a 10% neutral density filter placed in the excitation beam. Fluorescein and rhodamine were quantified by using 488- and 514-nm laser lines and excitation cubes with 510-nm dichroic/515-nm barrier filter and 580-nm dichroic/580-nm barrier filter combinations, respectively. Rhodamine emission was further excluded from fluorescein images by placing a 575-nm short-pass dichroic and a 530 ± 15-nm bandpass filter in the emission light path. A 40× oil-phase objective was used to focus the laser beam to a $1/e^2$ radius of 1.3 μm at the sample plane. The stage was moved over a $60 \times 60\ \mu m^2$ area in 0.5-μm steps; fluorescence at each location was monitored by a photomultiplier tube and digitized by the computer. The distribution of fluorescence intensities in each scanned field was displayed as a 4095-model-color two-dimensional image. Three types of samples were analyzed. The experimental sample (GVHD) was GVHD mouse skin stained with unlabeled primary antibodies (directed against both CD3 and CD4) and fluorescently labeled secondary antibodies ($n = 39$ cells analyzed). The negative control was identical to the experimental sample, except that the primary antibody directed against CD3 was omitted ($n = 24$ cells). The positive control was normal mouse skin stained identically to the experimental sample ($n = 29$ cells). $CD4^+$ cells in GVHD skin and $CD3^+$ cells in normal skin were identified visually by using full-field illumination by a mercury arc lamp. After laser scanning of each field, ACAS software was used to draw polygons around the boundaries of fluorescently labeled cells. Data were recorded as the difference between the average CD3 fluorescence intensity inside and outside each cell boundary. Since there were no significant differences among polygon areas in the three types of samples, differences in CD3 intensity are not attributable to an effect of altered cell size.

Isolation of Skin Lymphocytes. Ears are rinsed in alcohol and split with a watchmaker's forceps. The skin is then floated dermal side down on a 0.5% solution of trypsin (United States Biochemical) in PBS (Whittaker Bioproducts) for 40 min at 37°C. The loosened epidermis is removed and placed in a solution of 0.05% DNase (Sigma) in PBS at room temperature for an additional 20 min. The epidermis is then teased apart with forceps in Hanks' balanced salt solution (HBSS; GIBCO) that contains 10% fetal calf serum (FCS) (Whittaker Bioproducts) to produce a single cell suspension, filtered through nylon mesh, and washed three times in HBSS with 10% FCS. The viability of the epidermal cells in these suspensions ranges between 85% and 90%, as determined by trypan blue exclusion. To enrich for lymphocytes, epidermal cell suspensions are fractionated on a Ficoll/Hypaque density gradient. Epidermal cells (5×10^6 per ml) are layered onto 3 ml of lymphocyte separation medium (Organon Teknika–Cappel) and centrifuged at $400 \times g$ for 30 min at 10°C. Epidermal cells at the interface are harvested and washed three times in HBSS with 10% FCS. The yield of viable epidermal cells recovered ranges between 2% and 5% of total epidermal cells layered onto the gradient.

RESULTS

We analyzed the cell surface phenotype of lymphocytes infiltrating the skin of mice with GVHD in two murine bone marrow transplant models (B10.BR → CBA, B10.BR → AKR). We induced GVHD by transplanting a mixture of T cell-depleted B10.BR bone marrow cells and T cells into lethally irradiated (1100 cGy) CBA and AKR mice as described (7). Donor and recipient strains are congenic at the major histocompatibility complex ($H\text{-}2^k$) but differ at multiple minor histocompatibility loci and thus reflect the genetics of *HLA*-identical allogeneic bone marrow transplantation. Mice identically transplanted with T cell-depleted bone marrow served as non-GVHD controls.

To evaluate the potential role of dendritic epidermal cells in GVHD, we analyzed the phenotype of lymphocytes in the epidermis during the first 3 weeks after transplant (Fig. 1). Murine epidermis normally contains a subclass of $Thy\text{-}1^+$ T lymphocytes that are $CD3^+$ $CD4^-$ $CD8^-$ and bear the $\gamma\delta$ T-cell receptor (13–15). We have found that during this period, lymphocytes of an unusual phenotype ($CD4^+$ $CD8^-$ $CD3^-$) appear in the epidermis. Analysis of the epidermis of transplanted mice without GVHD showed a transient decrease in resident $CD3^+$ $CD4^-$ $CD8^-$ cells and a return of these cells by day 16 (Fig. 1*A*). In contrast, $CD3^+$ cells disappeared by day 13 and did not recover in the skin of mice with GVHD; however, a $CD4^+$ cellular infiltrate was detected (Fig. 1*B*). $CD8^+$ cells were not present in the skin from mice with GVHD, and neither $CD4^+$ nor $CD8^+$ cells were present in the epidermis of transplanted mice without GVHD.

The skin of mice with GVHD was examined for several additional lineage markers (Fig. 2). We first used double exposures of two-color immunofluorescence of CD3 and CD4 antigens to distinguish resident dendritic epidermal cells from cells infiltrating the epidermis of mice with GVHD. Resident $CD3^+$ (FITC) epidermal lymphocytes were observed on day 8 after transplant, and as expected, these cells did not express CD4 (Fig. 2*A*). They were also $V_\gamma 3^+$ and therefore expressed the $\gamma\delta$ T-cell receptor (data not shown). Surprisingly, the $CD4^+$ cells (orange) did not express the CD3 antigen, although $CD4^+$ cells in normal thymus and spleen did express CD3 and appeared yellow on

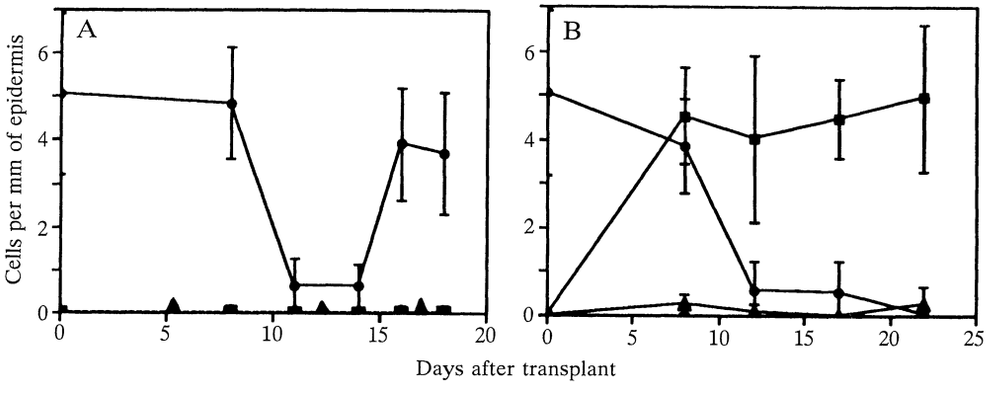

FIG. 1. T-lymphocyte phenotypes in mouse epidermis after bone marrow transplant. CBA mice were transplanted with 10^7 T-cell-depleted B10.BR bone marrow cells alone (*A*) or with 10^7 T-cell-depleted B10.BR bone marrow cells and 10^6 B10.BR splenic T cells (*B*). Ear skin was harvested on the days indicated and stained with anti-CD3, anti-CD4, and anti-CD8 monoclonal antibodies. $CD4^+$ cells (■) appear only in GVHD skin (*B*). Six to eight sections were scored per sample. The number of positive cells in the epidermis are expressed as M ± SD. ●, $CD3^+$; ▲, $CD8^+$.

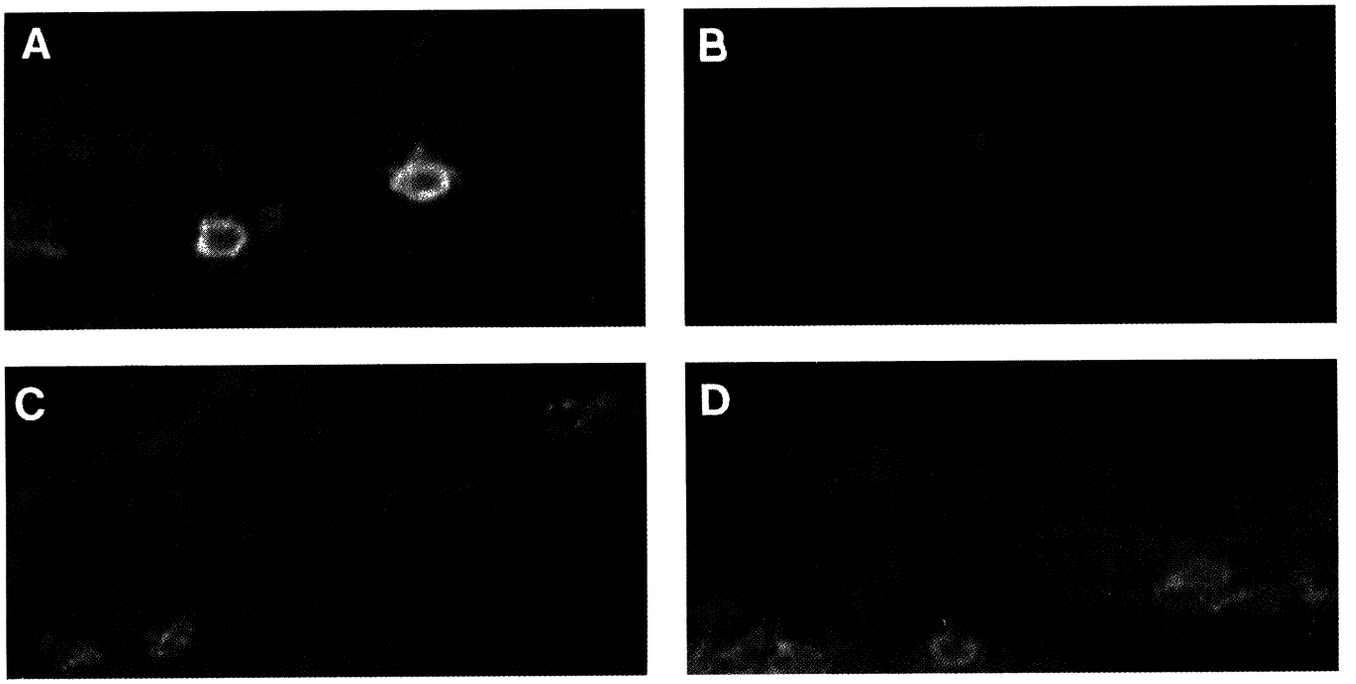

FIG. 2. Lymphocytes infiltrating skin of mice with GVHD have a $CD3^-$ $CD4^+$ $CD2^+$ Thy-1^+ phenotype. GVHD was induced in CBA mice (*A–C*) and AKR mice (*D*) by transplantation of B10.BR bone marrow cells and T cells as described. Double exposure of ear skin from days 8 (*A*) and 19 (*B*) identifies cells labeled with anti-CD4 in orange and with anti-CD3 in yellow-green. Single exposure of *A* under green filters alone identifies yellow-green ($CD3^+$) cells as green but does not visualize $CD4^+$ cells (data not shown). Skin from day 19 was also analyzed by single-color (green) immunofluorescence and shows cells labeled with anti-CD2 (*C*) and donor-specific anti-Thy-1.2 (*D*). (×400.)

double exposure (data not shown). By day 19 after transplant, $CD4^+$ cells were the predominant lymphocyte in the epidermis, and $CD3^+$ cells were no longer observed (Figs. 1*B* and 2*B*). Analysis of additional T-cell antigens showed that infiltrating cells expressed Thy-1 and CD2 (Fig. 2 *C* and *D*). CD2 is expressed on murine B cells (16) but these cells are immunoglobulin negative and therefore not of B lineage (data not shown). The CD4 antigen has been detected on human monocytes (17,

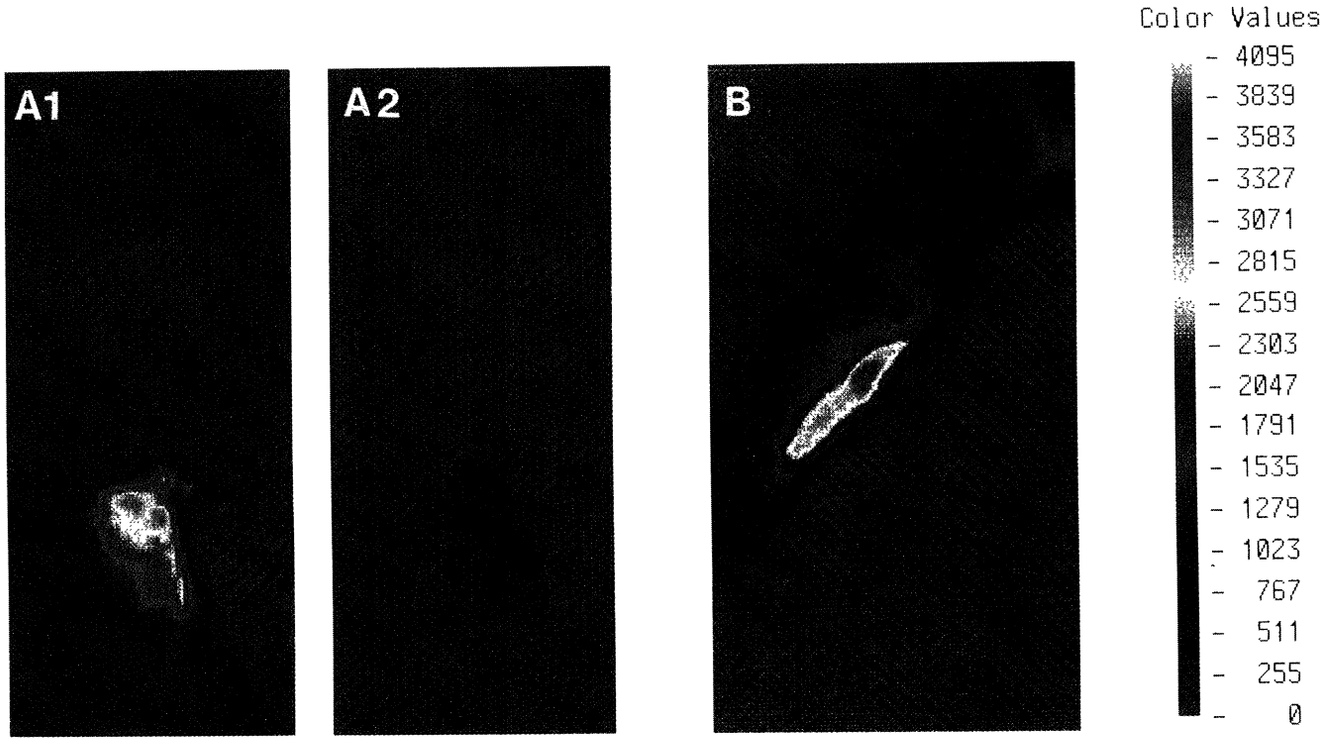

FIG. 3. Pseudo-color images of fluorescence intensity of skin lymphocytes. Tissue sections from GVHD (*A*) and normal (*B*) skin were labeled with anti-CD4 (*A1*) and anti-CD3 (*A2* and *B*) as described in Fig. 2. The same frame of GVHD skin was analyzed for fluorescence of CD4 (*A1*) and CD3 (*A2*). Images were collected by using the ACAS 570 interactive laser cytometer. Fluorescence intensity color values are shown in the scale on the right.

18), but the cells that we observed during GVHD did not express antigens that are characteristic of macrophages or dendritic Langerhans cells (measured by lack of anti-Ia and F/480 staining; data not shown). We also analyzed these cells for markers of natural killer lineage because large granular lymphocytes have been implicated as effectors of GVHD in this murine model (7, 8). $CD4^+$ lymphocytes in GVHD skin were uniformly $NK1.1^-$, and thus not typical natural killer cells, although ≈40% were asialoganglioside GM_1 positive (data not shown).

We investigated GVHD in a second strain combination (B10.BR → AKR) in which we could determine whether the infiltrating T lymphocytes were of donor (Thy-1.2) or of host (Thy-1.1) origin. $CD4^+$ $CD8^-$ $CD3^-$ cellular infiltrates were again observed only in mice with GVHD (data not shown). Directly labeled anti-Thy-1.2-FITC, which detects only donor cells, stained the infiltrating cells and confirmed their T-cell lineage as well as their donor origin (Fig. 2*D*).

The absence of the CD3 antigen in these donor-derived $CD4^+$ T cells was an unexpected observation. We performed digital image analysis of immunofluorescence using an interactive laser cytometer (19) to measure precisely the level of CD3 expression on these cells. This approach has several advantages: CD3 expression can be quantified *in situ* without disruption of the tissue; instrument parameters can be adjusted to maximize sensitivity to changes in fluorescence intensity; and results are quantitative as well as qualitative, permitting comparisons between cells in sequential tissue sections. Skin from mice with GVHD was stained for both CD4 and CD3, $CD4^+$ cells were identified visually, and the laser cytometer was used to analyze the same cells for CD3 fluorescence (Fig. 3*A*). Two monoclonal antibodies directed against the CD3 ε chain (145-2C11, 500-AA2) were used for staining. There was no detectable specific CD3 ε chain expression in the large majority (30 of 39 = 77%) of cells in skin from mice with GVHD. Cells with a $CD3^-$ $CD4^+$ phenotype are thus the predominant lymphocyte (approximately four cells per mm) in affected epidermis. All assays were performed on frozen tissue sections and therefore measure (and cannot distinguish between) cytoplasmic and cell surface immunofluorescence. Thus it is highly unlikely that CD3 has simply modulated from the cell surface, because these techniques would also detect CD3 in the cytoplasm.

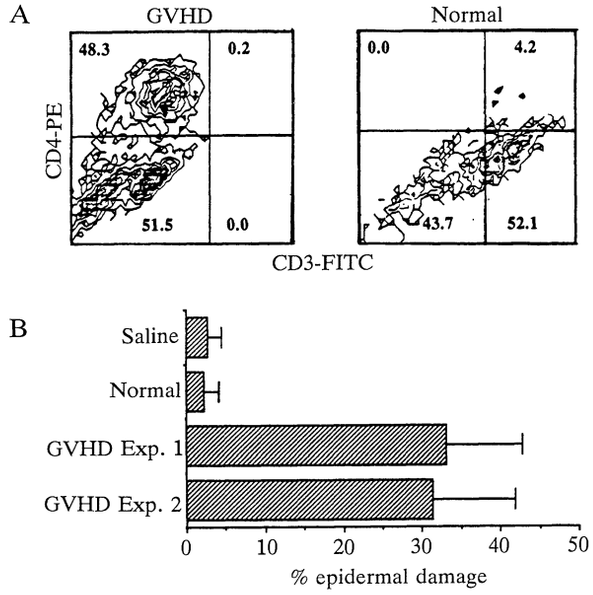

FIG. 4. $CD4^+$ $CD3^-$ GVHD lymphocytes cause epidermal damage. (*A*) Two-color immunofluorescence of isolated skin lymphocytes. Lymphocytes were isolated from the epidermis of normal mice (*Right*) and mice with GVHD 18 days after transplant (*Left*). Cells were then stained with FITC-conjugated anti-CD3 and phycoerythrin (PE)-conjugated anti-CD4, and 5000 cells were analyzed on a FACScan. (*B*) Epidermal damage caused by adoptive transfer of skin lymphocytes to secondary recipients. Skin lymphocytes were isolated as in *A* and injected intradermally into secondary CBA recipients that had received 900 cGy total body irradiation. Five days later, skin was taken, and epidermal damage was measured by scoring the separation of epidermis from the dermis.

To determine the function of $CD4^+$ $CD3^-$ lymphocytes, we first isolated them from the skin of mice with GVHD and performed two-color immunofluorescence by fluorescence-activated cell sorting analysis (Fig. 4*A*). Approximately half of the mononuclear cells isolated from the skin of mice with GVHD possessed the $CD4^+$ $CD3^-$ phenotype; the remaining 50% were double negatives and probably represent keratinocytes included in the mononuclear cell preparation. These keratinocytes also represented about 50% of the cells in the preparation of epidermal lymphocytes from normal skin; the remaining lymphocytes in normal skin were $CD3^+$ $CD4^-$, as expected. We next transferred these lymphocytes into the skin of secondary irradiated recipients to determine whether they could mediate the epidermal damage characteristic of GVHD (Fig. 4*B*). Injection of $CD3^+$ cells from normal skin caused minimal damage, which was no greater than that caused by the injection of saline. By contrast, injection of $CD4^+$ $CD3^-$ cells from GVHD skin caused significant epidermal damage in two separate experiments (GVHD experiments 1 and 2). Thus, $CD4^+$ $CD3^-$ lymphocytes can act as effector cells of cutaneous GVHD.

DISCUSSION

These results show that the predominant lymphocyte population in the epidermis of mice with GVHD are donor-derived cells with an unusual phenotype. These cells possess several T-cell lineage markers (Thy-1, CD2, CD4) but do not express CD3 or CD8. Although a very low level of CD3 or CD8 expression cannot be excluded by these techniques, such expression is below the level detectable by fluorescent antibodies and sensitive digital image analysis.

It is not yet clear whether these $CD4^+$ $CD8^-$ $CD3^-$ cells are of thymic origin or whether they develop in a completely extrathymic environment. Only recently has the $CD4^+$ $CD8^-$ $CD3^-$ phenotype been recognized as a stage of T-cell development. The $CD4^+$ $CD8^-$ $CD3^-$ population comprises ≈1% of normal thymocytes and ≈10% of all $CD4^+$ thymocytes, but it is not found in lymph nodes (9). These $CD4^+$ cells appear to be the earliest thymocyte precursors yet isolated and are more prominent during fetal ontogeny and during thymic reconstitution after bone marrow transplantation, where they may be 6% of the total thymocyte population (10–12).

Our data show that during the immunopathophysiological events of GVHD, the $CD4^+$ $CD8^-$ $CD3^-$ phenotype is more than an early stage of thymocyte development. This population is expanded in peripheral tissues and is *the* predominant lymphocyte population in the skin during the first 3 weeks of a graft-versus-host reaction, where it causes target destruction. The amplification and activation of these cells may be due to both the damage inflicted on thymic epithelium (20–22) and to proliferative stimuli supplied by dysregulated production of lymphokines such as γ interferon and tumor necrosis factor (23, 24). A damaged thymus has been shown to be essential to the effector mechanism of GVHD in other models, particularly in syngeneic GVHD, where the normal balance between autoregulatory and autoaggressive cells is altered (25). Dysregulated cytokines are also likely to contribute to the effector function of these lymphocytes. Such cytokines may not only activate them but also alter their expression of homing receptors for GVHD target organs.

We thank J. P. Allison and A. Ezekowitz for their gifts of antibodies; I. Rimm and S. Goldman for helpful discussions; Linda

Brown for secretarial assistance; and M. Brenner, B. Sleckman, and B. Mathey-Prevot for reviewing the manuscript. This work was supported by grants from the National Institutes of Health, the American Cancer Society, and the Dyson Foundation.

1. Korngold, R. & Sprent, J. (1978) *J. Exp. Med.* **148,** 1687–1698.
2. Vallera, D. A., Soderling, C. C. B., Carlson, G. J. & Kersey, J. H. (1981) *Transplantation* **31,** 218–226.
3. Sprent, J., Schaeffer, M., Gao, E.-K. & Korngold, R. (1988) *J. Exp. Med.* **167,** 556–569.
4. Rolink, A. G. & Gleichmann, E. (1983) *J. Exp. Med.* **158,** 546–558.
5. Hale, G., Cobbold, S. & Waldmann, H. (1988) *Transplantation* **45,** 753–759.
6. Ferrara, J. L. M. & Deeg, H. J. (1991) *N. Engl. J. Med.* **324,** 667–674.
7. Ferrara, J. L. M., Guillen, F. J., van Dijken, P. J., Marion, A., Murphy, G. F. & Burakoff, S. J. (1989) *Transplantation* **47,** 50–54.
8. Ferrara, J., Guillen, F. J., Sleckman, B., Burakoff, S. J. & Murphy, G. F. (1986) *J. Invest. Dermatol.* **86,** 371–375.
9. Hugo, P., Waanders, G. A., Scollay, R., Shortman, K. & Boyd, R. L. (1990) *Int. Immunol.* **2,** 209–218.
10. Matsumoto, K., Yoshikai, Y., Matsuzaki, G., Asano, T. & Nomoto, K. (1989) *Eur. J. Immunol.* **19,** 1203–1207.
11. Mosley, R. L. & Klein, J. R. (1991) *Transplantation*, in press.
12. Wu, L., Scollay, R., Egerton, M., Pearse, M., Spangrude, G. J. & Shortman, K. (1991) *Nature (London)* **349,** 71–74.
13. Koning, F., Stingl, G., Yokoyama, W. M., Yamada, H., Maloy, W. L., Tschachler, E., Shevach, E. M. & Coligan, J. E. (1987) *Science* **236,** 834–836.
14. Kuziel, W. A., Takashima, A., Bonyhadi, M., Bergstresser, P. R., Allison, J. P., Tigelaer, R. E. & Tucker, P. W. (1987) *Nature (London)* **328,** 263–266.
15. Romani, N., Stingl, G., Tschachler, E., Witmer, M. D., Steinman, R. M., Shevach, E. M. & Schuler, G. J. (1985) *J. Exp. Med.* **161,** 1368–1383.
16. Yagita, H., Nakamura, T., Karasuyama, H. & Okumura, K. (1989) *Proc. Natl. Acad. Sci. USA* **86,** 645–650.
17. Maddon, P. J., Molineaux, S. M., Maddon, D. E., Zimmerman, K. A., Godfrey, M., Alt, F. W., Chess, L. & Axel, R. (1987) *Proc. Natl. Acad. Sci. USA* **84,** 9155–9159.
18. Wood, G. S., Warner, N. L. & Warnke, R. A. (1983) *J. Immunol.* **131,** 212–216.
19. Moutsatsos, I. K., Wade, M., Schindler, M. & Wang, J. L. (1987) *Proc. Natl. Acad. Sci. USA* **84,** 6452–6456.
20. Ghayur, T., Seemayer, T. A. & Lapp, W. S. (1989) *Clin. Immunol. Immunopathol.* **48,** 19–30.
21. Fukuzawa, M., Via, C. S. & Shearer, G. M. (1988) *J. Immunol.* **141,** 430–439.
22. Ferrara, J. L. M., Daley, J. P., Burakoff, S. J. & Miller, R. A. (1987) *J. Immunol.* **138,** 3598–3603.
23. Wall, D. A., Hamberg, S. D., Reynolds, D. S., Burakoff, S. J., Abbas, A. K. & Ferrara, J. L. M. (1988) *J. Immunol.* **140,** 2970–2976.
24. Piguet, P. F., Gran, G. E., Allet, B. & Vassali, P. (1987) *J. Exp. Med.* **166,** 1280–1289.
25. Fischer, A. C., Beschorner, W. E. & Hess, A. D. (1989) *J. Exp. Med.* **169,** 1031–1042.